NUREG/CR-1785
UCRL-53012

Performance Evaluation of Loss Detection Schemes for Uranium Recovery Plants

D. T. Gavel

Prepared for
U.S. Nuclear Regulatory Commission

LAWRENCE
LIVERMORE
LABORATORY

Available from

GPO Sales Program
Division of Technical Information and Document Control
U. S. Nuclear Regulatory Commission
Washington, D. C. 20555

Printed copy price: $4.25

and

National Technical Information Service
Springfield, Virginia 22161

NUREG/CR-1785
UCRL-53012
RS

Performance Evaluation of Loss Detection Schemes for Uranium Recovery Plants

Manuscript Completed: November 1980
Date Published: November 1981

Prepared by
D. T. Gavel

Lawrence Livermore Laboratory
7000 East Avenue
Livermore, CA 94550

Prepared for
Office of Nuclear Regulatory Research
U.S. Nuclear Regulatory Commission
Washington, D.C. 20555
NRC FIN No. A0115

ACKNOWLEDGMENTS

The author wishes to thank J. Candy and D. Dunn for their technical discussions and helpful review of this report. R. Rozsa provided invaluable assistance with the chemical engineering details. Special thanks are due to I. Morris and M. Hamilton for typing this report.

ABSTRACT

This report presents four loss detection schemes for special nuclear material (SNM) accounting at a typical uranium recovery facility. We conceptually define a detector and discuss loss detector performance evaluation criteria. The loss detection schemes are evaluated for a hypothetical SNM loss scenario. The schemes presented are (1) material balance accounting (MBA), where single measurements are made of incoming and outgoing SNM; (2) MBA, augmented by additional measurements (i.e., multiple instruments) made on chemical processes within the plant; (3) augmented MBA, with the measurement instruments improved by multiple independent reading; and (4) a detector based on a parameterized model of the chemical process. The results of our analysis show that better process models and improved accuracy measurements can greatly enhance the performance of an SNM diversion detector. Detector performance was evaluated for an 8-hour batch processing time.

CONTENTS

LIST OF ILLUSTRATIONS

LIST OF TABLES

Chapter 1

INTRODUCTION

The safeguarding of special nuclear material (SNM) continues to be of vital importance to the nation. The attractiveness of weapons grade SNM to terrorist organizations presents a grave danger to the general public. Unfortunately, existing methods of material balance accounting (MBA) in nuclear fuel reprocessing plants may be inadequate for timely detection of the loss of significant amounts of SNM; therefore, it is necessary to investigate alternative methods.

This report presents some simple signal processing techniques that can enhance the probability of detecting a loss of SNM. A model facility is used as an example of a nuclear fuel reprocessing plant in which to characterize our loss detection schemes.

Signal processing techniques involve the monitoring of process variables inside the chemical plant and the analysis of data using a process model. MBA is an example of a simple signal processing technique, viz., SNM input and output are compared. Statistical techniques[1] are used to determine if SNM diversion has occurred. In an MBA scheme, the chemical process dynamics inside a plant are not modeled.

We are presenting detection schemes that utilize more process information than traditional MBA. Figure 1.1 shows a "staircase" of models that can be used in a loss detection scheme. In this report, we discuss two improved-accuracy input/output (MBA) models and one parameter model. These correspond to the first two levels of process models in the staircase. We then develop three detection schemes and characterize their performance, in comparison to the MBA scheme, in a hypothetical diversion scenario for the model facility. Future work will cover the reduced order and true process models, the third and fourth levels of process modeling.

The improved accuracy MBA and parameter models offer improved detection performance over simple MBA schemes in the sense that probability of detecting an SNM loss is increased. The higher level models have an additional advantage of timeliness because they are dynamic process models coupled with on-line monitors.

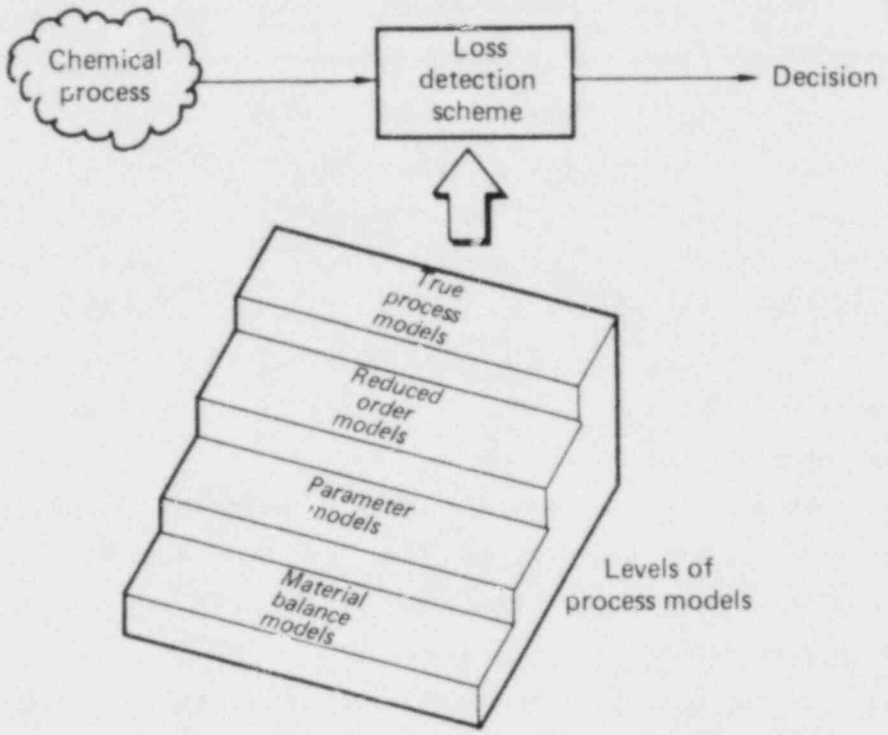

FIG. 1.1. Classes of process models.

Chapter 2 of this report discusses the general properties of a detector, defines some terms, and introduces performance evaluation criteria. Chapter 3 gives a brief description of a model uranium recovery plant that is used in a hypothetical SNM diversion scenario.

In Chapter 4, four detection schemes are evaluated for the hypothetical scenario. Each succeeding scheme presented has a better process model or uses more accurate measurements than the previous scheme, and thereby offers improved performance, as shown in the report. The four schemes presented include the following: (1) material balance accounting (MBA), where single measurements are made of incoming and outgoing SNM; (2) MBA, augmented by additional measurements (i.e., multiple instruments) made on chemical processes within the plant; (3) augmented MBA, with the measurement instruments improved by multiple independent readings; and (4) a detector based on a parameterized model of the chemical process.

In the hypothetical scenario discussed in the report, if 1 kg of SNM is stolen, the MBA scheme can only hope to detect the loss with a probability of

0.2 (this is assuming a false alarm probability of 0.05). The multiple instrument, multiple measurement, and parameter model schemes have detection probabilities of 0.4, 0.97, and 0.99, respectively (also assuming a false alarm probability of 0.05). These results are derived in detail in the report and are valid for an 8-hour batch processing time period. Therefore, we can conclude that better process models and improved accuracy measurements can greatly enhance the performance of an SNM diversion detector.

A summary of results is presented in Chapter 5. Chapter 6 gives some suggestions for future work.

Chapter 2

DETECTORS

The detection schemes described in this report all fit within the realm of binary hypothesis testing. This chapter defines binary hypothesis testing, and it describes how to characterize the performance of a binary detector. Appendix A gives a mathematical review of detection theory since this chapter gives only a brief presentation of basic concepts. Section 2.2 describes how, in terms of hardware, a detector would be put on-line at a nuclear processing facility.

2.1 PROPERTIES OF DETECTORS

A binary detector uses all the information available to it to make a choice between two possible outcomes or "hypotheses," hence the term "binary hypothesis test." The two hypotheses in our case are (1) H_o: all the SNM is accounted for; and (2) H_1: some SNM is missing. As a general rule, the more accurate the information given, the better the detector performs. How do we quantify performance? What makes one detector better than another? We define three important measures of detector performance: probability of detection, probability of false alarm, and time to detection.

The probability of detection is a measure of how likely it is that an alarm will trigger when a diversion occurs. We would like this probability to be in the 0.95 to 1 range, but in designing a detector for maximum detection probability, the false alarm rate must be kept low. False alarm probability* is a measure of how often the alarm is triggered when in fact no diversion occurred. In a practical diversion detection scheme, false alarm probability is usually constrained to about 0.05 (5 percent). The solution to the problem of maximizing probability of detection under a false alarm probability constraint is the so-called "likelihood ratio" detector (Appendix A). The detectors described in this report are all likelihood ratio detectors.

Another important quality of a detector is timeliness. Time to detection is the (average) time lag from diversion to detection. For the detectors

---

*The terms rate and probability are interchangeable here. To be precise, the rate is the probability divided by the sampling interval. The sampling interval here is the batch process time, 8 hours.

described in this report, the time lag can be anywhere from 0 to 8 hours because the accounting does not take place until after an 8-hour long batch process. A timely detector would be an on-line detector that monitors a chemical processing unit during the batch process and warns of the diversion most nearly after the event as possible.

Let us return to the criterion of probability of detection. We have fixed the false alarm probability at a certain value. We now discuss what factors contribute to an increased probability of detection.

The probability of detecting SNM loss is a function of the signal-to-noise ratio (SNR), as shown in Fig. 2.1.* The signal is the amount of lost SNM, and the noise is our uncertainty (standard deviation) in the total amount of SNM lost.

The SNR performance curve can prove useful to an NRC regulator/assesssor. For example, suppose the total plant uncertainty is characterized by the standard deviation σ_1, then for a given loss (signal) of material, S, the detection probability is fixed, say P_1 (Fig. 2.1). If the regulator

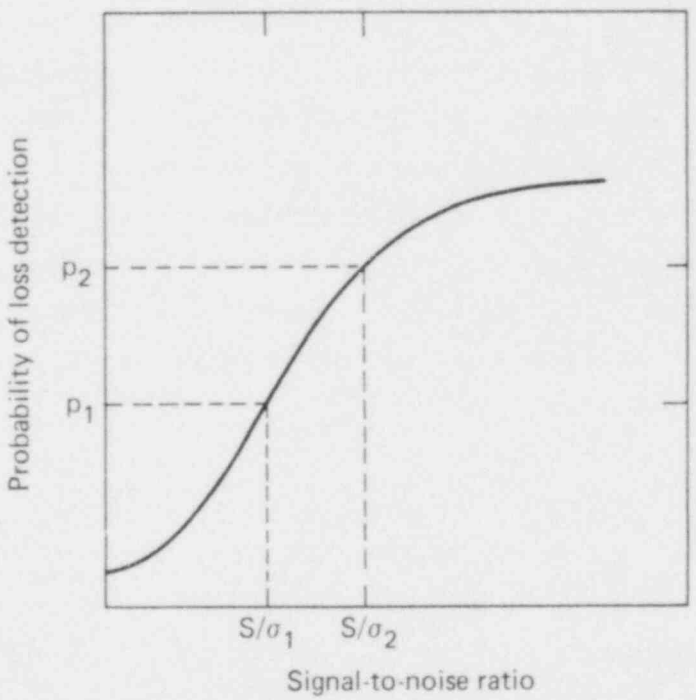

FIG. 2.1. Probability of detection vs signal-to-noise ratio.

*This function is derived mathematically in Appendix A.

required a higher detection probability for the same loss, S, then the plant uncertainty must decrease; i.e., $\sigma_2 < \sigma_1$ for $P_2 > P_1$. If σ_2 is impractical, then the regulator knows that P_2 is not realistic. Other similar scenarios could be imagined. Thus, the performance curve, along with cost information to indicate the feasibility of reducing σ_1 to σ_2 (e.g., improved measurements), will prove to be a powerful "nomogram" for the NRC.

In Chapter 4, we evaluate the performance of detectors by plotting points on the performance evaluation curve for each example detection scheme.

2.2 DETECTOR IMPLEMENTATION AT A PROCESSING PLANT

We have conceptually described how to characterize a diversion detector. Let us now explain physically what a detector may look like when implemented at a nuclear fuel reprocessing plant.

The detector system complexity depends on the complexity of the process model in the scheme (Fig. 1.1). A material balance accounting system may simply be an accountant with pencil and paper; however, the more complicated models require a computer to perform the required calculations reliably. A fully automated system would use a minicomputer (or microprocessor) electronically interfaced to the measurement instruments. Many instruments used in reprocessing plants already have interfaces built in, such as the Ruska-Taylor pressure sensors, which have an electrical output signal. The computer provides all the computations necessary to make a decision. The output is merely a "yes" or a "no," plus perhaps an estimate of how much material was stolen (loss estimate) and from what part of the plant the theft occurred (localization estimate).

Chapter 3

MODEL URANIUM PROCESSING FACILITY

We wish to evaluate signal processing techniques for SNM loss detection for a model nuclear material recovery facility. To do this we first describe the operation of the model facility and then explain the techniques for measuring the amount of SNM present at various processing stages within that facility. We next perform an error analysis for the measurement schemes, and we investigate the sources of normal, in-process, SNM loss. The results of the error and loss analysis are used in Chapter 4 to characterize loss detector performance at the model plant.

3.1 PLANT OPERATION

The purpose of the model plant is to extract and purify uranium from fuel rods. Figure 3.1 outlines the process. As fuel rods enter the plant, they are ground up and dissolved in nitric acid. Pulse columns extract the uranium solution and the resulting 6 kg/m^3 uranium nitrate is stored in tanks. These tanks feed solution to the concentrator unit where the solution density is increased from 6 kg/m^3 to 100 kg/m^3. The concentrate is stored in a tank until ready for precipitation. The precipitator is used to convert the concentrated solution to solid form.

The concentrator/precipitator section has four chemical units of interest (Fig. 3.2): (1) storage tanks for low-concentration uranium nitrate solution, (2) a concentrator unit, (3) a storage tank for high-concentration uranium

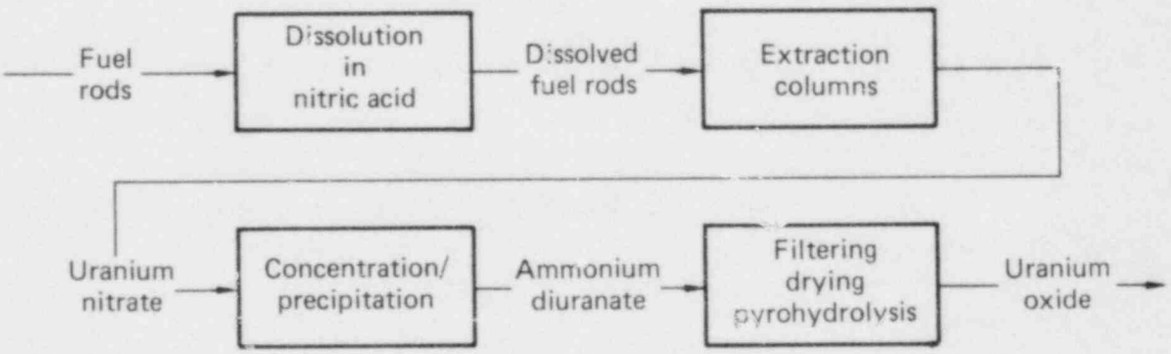

FIG. 3.1. Uranium purification process.

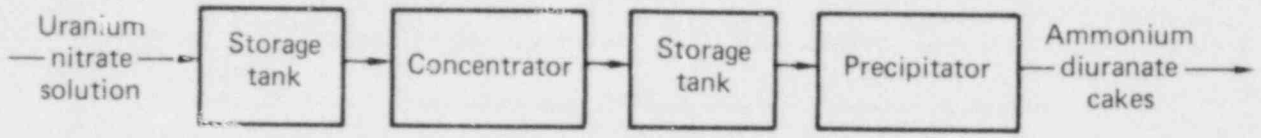

FIG. 3.2. Concentration/precipitation stages.

nitrate solution, and (4) a precipitator unit. Volumes and batch process times for each unit are summarized in Table 3.1.

Let us first discuss the concentrator and precipitator units in more detail since we are concerned with measurements on the processes in these units.

3.1.1 Concentrator Unit

The concentrator is shown in Fig. 3.3. At the start of a batch process, it is filled with about 0.05 m^3 of 6 kg/m^3 uranium nitrate solution. The solution is heated by steam in a reboiler.

Nitric acid evaporates, thus increasing the solution concentration. The liquid level is held constant by a continuous incoming stream of 6 kg/m^3 solution from the feed tank. The concentration continuously increases until (about 7 hours later) the concentration has reached 100 kg/m^3. At this time, the feed is shut off, and the batch of 100 kg/m^3 solution is pumped into overhead storage tanks. During a 16-hour, 2-shift period, two batches of SNM can be processed through the concentrator.

TABLE 3.1. Volumes and batch process times for model plant processing units.

Stage	Volume, m^3	Batch processing time, hr
1. Tanks	0.7	
2. Concentrator	0.05	7
3. Tank	0.17	
4. Precipitator	0.02	1

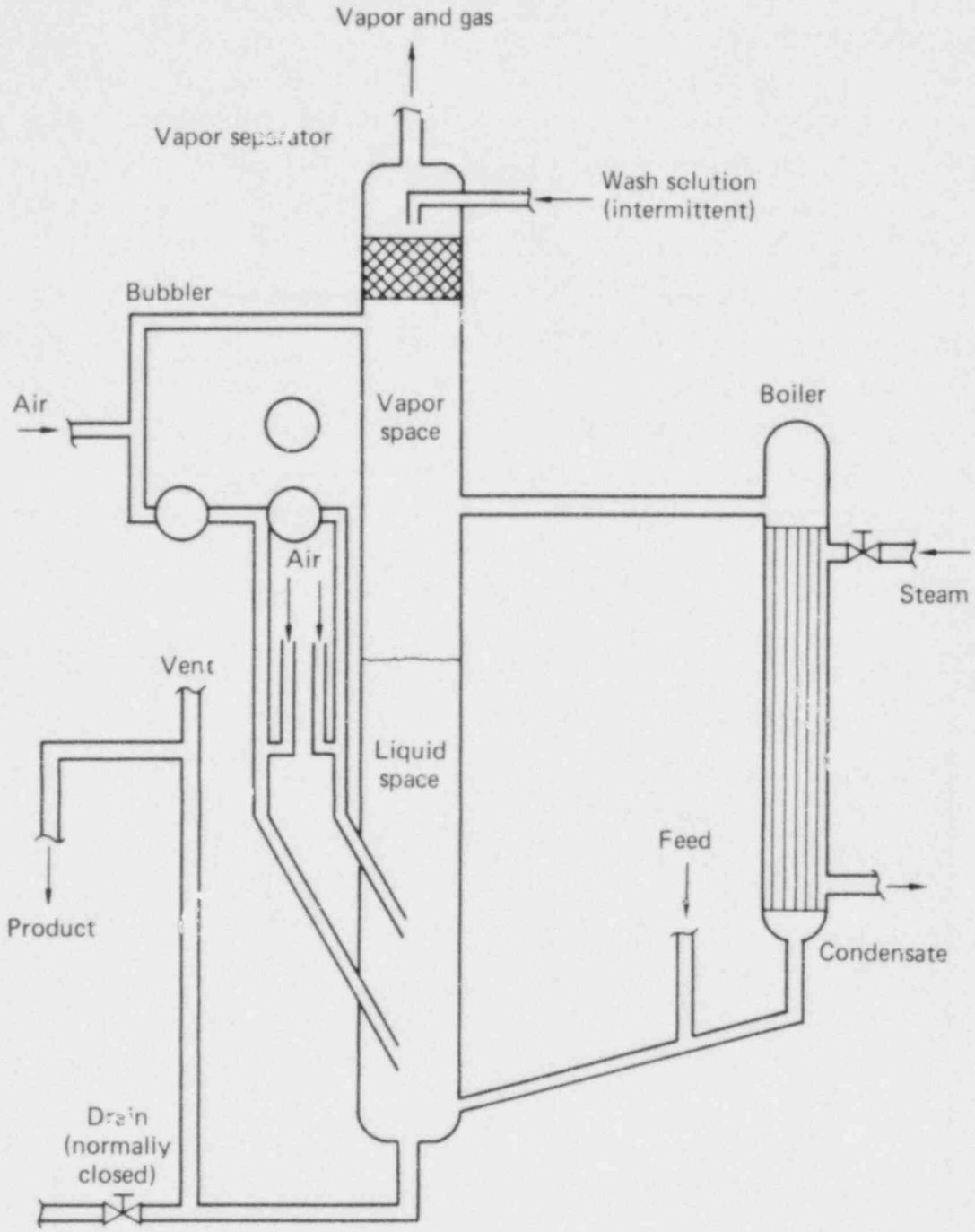

FIG. 3.3. Concentrator unit.

3.1.2 Precipitator Unit

Figure 3.4 shows the precipitator unit. The precipitator is smaller in volume than the concentrator, handling only about 0.02 m^3 of liquid at a time. Air and ammonia gas are bubbled through the precipitator full of the 100 kg/m^3 uranium nitrate solution. The reaction forms solid ammonium diuranate. At the end of 1-hour-long run, the precipitant is filtered-out and the remaining liquid discarded. The precipitant is a wet "cake," containing a high percentage of water, that is later dried and calcined to result in the final product, powdered uranium.

We now direct attention to the plant operating procedure and the techniques for determining the amount of SNM in various stages of the process.

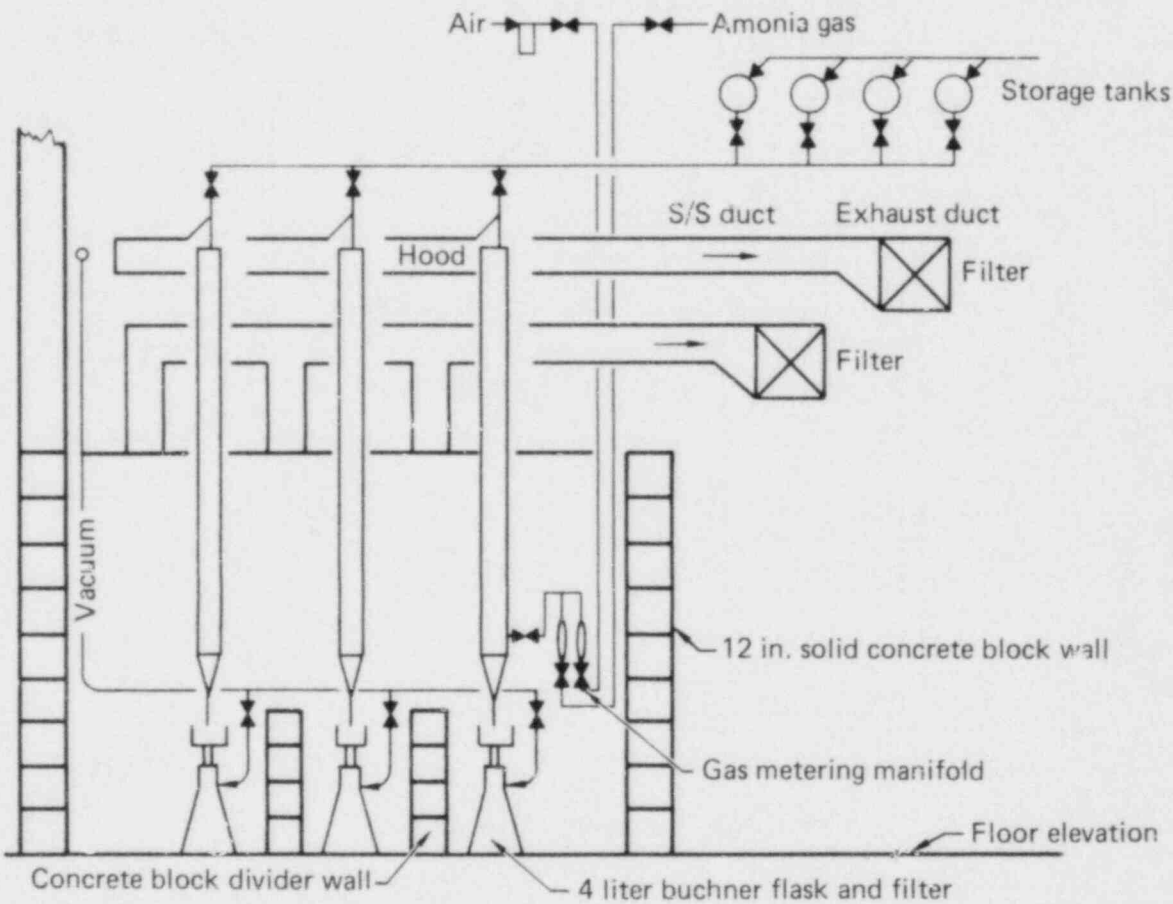

FIG. 3.4. Precipitator unit.

3.1.3 Plant Operating Procedure

To keep our investigation simple, we assume that the low-concentration liquid storage tanks are full before the concentrator runs are started. Precipitation is not started until all the concentrator runs are completed and stored in the high-concentration liquid storage tank. In this manner we have an easy way of keeping track of all the SNM during the batch processing.

3.1.4 Measuring SNM Content

In this section, we discuss methods of determining SNM content at four points in the concentration/precipitator process: (1) in the low-concentration uranyl-nitrate storage tanks; (2) in the SNM mass fed to the concentrator during a batch process; (3) in the SNM mass drained from the concentrator after batch process completion; and (4) in the cakes resultant from precipitation runs.

We have assumed that the storage tanks are filled before concentrator batch runs are performed; therefore, the volume of the tank determines the total amount of solution present and is easily calculated from its dimensions. In our model, that volume, V, is 0.7 m^3 (refer to Table 3.1). We further assume that there is some knowledge of the SNM concentration of the solution in the tank. In our model, that concentration, c, is 6 kg of SNM per cubic meter of solution. Thus, we can deduce the mass, M, of SNM in the storage tank:

$$M = cV \tag{3.1}$$

where

c = solution concentration (kg SNM/m^3 solution), and
V = tank volume (m^3).

In a second SNM mass measurement scheme, we use an existing instrument, a set of pressure gauges connected to bubbler tubes attached to the concentrator unit. Figure 3.5 shows the arrangement. The bubblers are useful for measuring two items: solution concentration (SNM density) and the liquid level inside the concentrator.

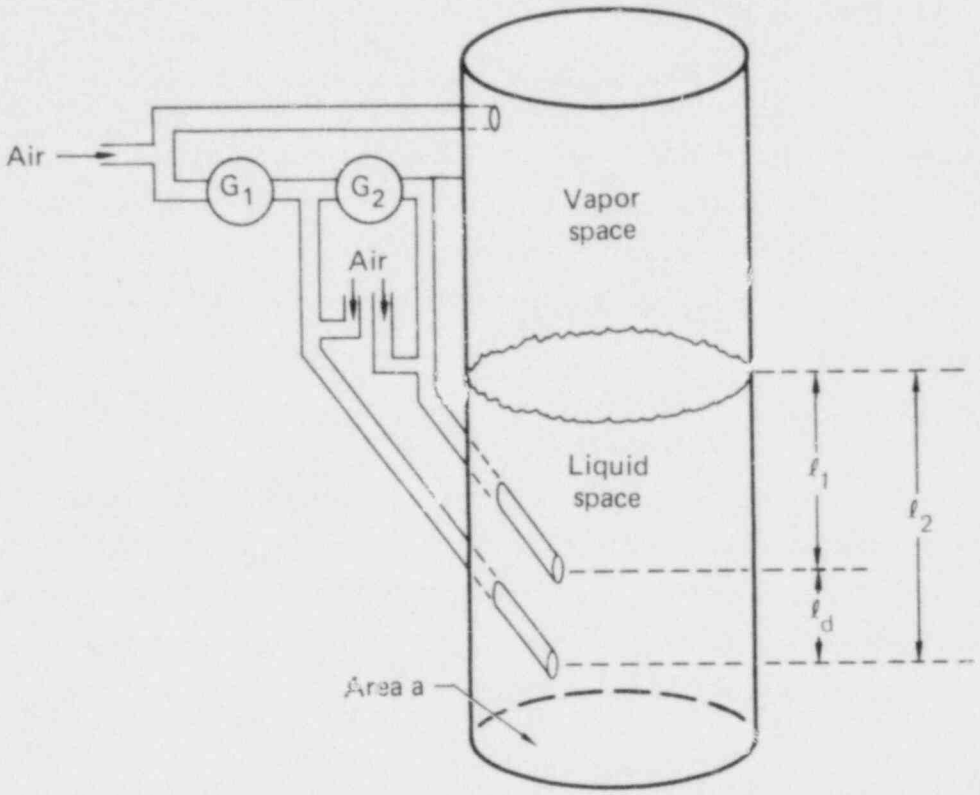

FIG. 3.5. Pressure gauge attachment to the concentrator unit.

Three bubbler tubes extend into the concentrator. Two tubes extend into the liquid space and one into the vapor space above the liquid.

The air pressure inside a particular bubbler tube is kept at equilibrium with the liquid (or vapor) pressure at the tube opening in the concentrator. Pressure gauges, G_1 and G_2, measure air pressure differential between the tubes. Gauge G_1 reads

$$P_1 = g\ \rho l_d \tag{3.2}$$

where

P_1 is pressure (nt/m^2),

g is the gravity constant (9.8 nt/kg),

ρ is the density of the liquid (kg/m^3), and

l_d is the bubbler tube height differential (m).

Since g and l_d are known and we measure p_1, we can compute the liquid density:

$$\rho = \frac{p_1}{g\, l_d} \tag{3.3}$$

Now Gauge G_2 reads

$$p_2 = g\, \rho l_2 \tag{3.4}$$

where l_2 is the level of the liquid with respect to the bottom bubbler tube. Therefore,

$$l_2 = \frac{p_2}{\rho g} \quad . \tag{3.5}$$

Substituting Eq. (3.3) into the above gives

$$l_2 = \frac{p_2}{p_1}\, l_d \quad . \tag{3.6}$$

To deduce the volume of liquid in the tank we need an accurate measurement of the "heel" space, that is, the liquid space below the lowest bubbler tube. Let us assume this has been previously measured to be V_h. So the total volume of liquid in the concentrator is

$$V = V_h + \frac{p_2}{p_1}\, l_d a \tag{3.7}$$

where a is cross-sectional area.

We can use the measurement of liquid density to deduce the concentration of SNM in the liquid. The concentration is <u>approximately</u> given by

$$c = \rho - \rho_s \tag{3.8}$$

where ρ_s is the density of the nitric acid solvent, i.e., the liquid density if no SNM were present. The approximation is valid in the range of concentrations we are interested in. For total SNM mass, multiply concentration by solution volume:

$$M = \left(\frac{P_1}{g\, l_d} - \rho_s\right)\left(V_h + \frac{P_2}{P_1}\, l_d a\right) \tag{3.9}$$

where

M = SNM mass in concentrator (kg),

P_1 = reading from pressure gauge G_1 (nt/m^2),

P_2 = reading from pressure gauge G_2 (nt/m^2),

ρ_s = density of the nitric acid solvent (kg/m^3),

g = gravity constant (9.8 nt/kg),

l_d = distance between bubbler tubes in the liquid space of the concentrator (m),

V_h = volume of the liquid space below the lowest bubbler tube (m^3), and

a = cross-sectional area of the concentrator above the lowest bubbler tube (m^2).

To measure the amount of SNM in the concentrator at the end of a batch run, we use the pressure readings P_1 and P_2 and Eq. (3.9).

We can also use the pressure gauges to help us determine the amount of SNM that enters the concentrator during the run (this may differ from the SNM mass in the concentrator at the end of the run because diversion may occur during processing). Initially, the concentrator is filled with low-concentration uranyl nitrate solution. At that time, we use Gauge G_1 to deduce the concentration of the solution stored in the tanks. Combining Eqs. (3.3) and (3.8) gives

$$c = \frac{P_1}{g\, l_d} - \rho_s \tag{3.10}$$

If we have some knowledge of the flow rate, f, of solution from the tanks into the concentrator (we will assume this is constant) and time, t, for the concentrator run (we assume that an accurate clock is available), we can compute the total SNM that flows into the concentrator:

$$M = cft = \left(\frac{P_1}{g\ l_d} - \rho_s \right) ft \qquad (3.11)$$

where

c = solution concentration (kg SNM/m^3 solution),

f = flow rate (m^3/sec),

t = time (sec),

P_1 = pressure reading from Gauge G_1 (nt/m^2),

g = gravity constant (9.8 nt/kg),

l_d = distance between bubbler tubes (m), and

ρ_s = density of nitric acid solvent (kg/m^3).

Our last SNM measurement scheme is the weighing of precipitant cakes. These cakes (ammonium diuranate) have a certain percentage of water and contaminants, so if we subtract the known amount of non-SNM weight we can deduce the amount of SNM present:

$$M = M_{cakes}\ (1-b) \qquad (3.12)$$

where

b = fraction of contaminants and water by weight.

We have now explained four methods of ascertaining SNM mass in the processing plant. We have computations for SNM in the storage tanks (3.1), SNM entering the concentrator (3.11), SNM leaving the concentrator (3.9), and SNM in the precipitant cakes (3.12).

3.2 ERROR AND LOSS ANALYSIS

We now consider the sources of SNM accounting uncertainty. We start by discussing sources of normal material loss within the plant (in-process losses). Then we analyze the sources of error introduced by the SNM measurement techniques explained in Section 3.1.4.

3.2.1 Normal Sources of Material Loss

Each chemical processing column, tank, and associated pipes and valves will be a source of SNM loss that is not necessarily a hostile diversion. For

example, some uranium may deposit onto the walls of a storage tank or there may be a small concentration in the liquid discarded from the precipitator column.

Experience may show that some certain average loss is to be expected, and hence can be accounted for in the final material balance. There is always some random variation around this average loss, so random loss must be included in the system model.

We assume that SNM loss uncertainties are relatively small compared to measurement errors. The assumed uncertainties for four types of loss at the model plant are shown in Table 3.2. The total loss uncertainty reflects the combination of all the random loss sources.

TABLE 3.2. Sources of in-process SNM loss.

Source	Percentage uncertainty, %	Equivalent SNM mass uncertainty, kg
Tank deposit	1	0.05
Vapor	3	0.15
Leakage	1	0.05
Discard	3	0.15
Total	4	0.2

3.2.2 Sources of Measurement Error

We now perform an error analysis* for each of the example SNM-measurement methods described in Section 3.1.4. The analysis will determine how measurement errors reflect in the uncertainty of SNM mass. We intend to use the results of the measurement error analysis in characterizing SNM loss detection schemes in Section 3.1.4.

Consider Eq. (3.1) for computing the mass, M, of SNM in the storage tanks:

$$M = cV \tag{3.13}$$

*See Appendix C for a mathematical derivation of the linear error analysis technique.

There is always some error in our guess of SNM concentration, c, and calculation of tank volume, V. Let us reflect that error in terms of the error in computing SNM mass:

$$\Delta M = (\Delta c)V + c(\Delta V) \tag{3.14}$$

In our development, it is more convenient to express these errors as fractions of their full-scale value:

$$\Delta M = \left(\frac{\Delta c}{c}\right) cV + \left(\frac{\Delta V}{V}\right) cV \tag{3.15}$$

or, since cV = M by Eq. (3.13),

$$\Delta M = M\left[\left(\frac{\Delta c}{c}\right) + \left(\frac{\Delta V}{V}\right)\right] \quad . \tag{3.16}$$

We now compute the variance of ΔM as

$$\boxed{\sigma_{ST}^2 = M^2 \left(\sigma_c^2 + \sigma_V^2\right)} \tag{3.17}$$

where

$\sigma_{ST}^2 = E\{\Delta M^2\}$ in the Storage Tank

$$\sigma_c^2 = E\left\{\left(\frac{\Delta c}{c}\right)^2\right\}$$

$$\sigma_V^2 = E\left\{\left(\frac{\Delta V}{V}\right)^2\right\}$$

In our model plant, we are assuming $\sigma_c = 0.1$, $\sigma_V = 0.1$ (i.e., the concentration and volume are determined with 10 percent uncertainty), and M = 5 kg. Therefore,

$$\sigma_{ST} = (5 \text{ kg}) \left[(0.1)^2 + (0.1)^2\right]^{1/2}$$

$$\sigma_{ST} = 0.71 \text{ kg} \quad . \tag{3.18}$$

The subscript ST indicates that we are talking about the variance of the SNM mass in the storage tanks.

The SNM mass being fed to the concentrator during a batch run is given by Eq. (3.11). Consider errors in the pressure reading, P_1, the flow rate, f, and time, t:

$$\Delta M = \left(\frac{\Delta p_1}{P_1}\right)\left(\frac{P_1}{gl_d}\right) ft + \left(\frac{\Delta f}{f}\right) M + \left(\frac{\Delta t}{t}\right) M \quad . \tag{3.19}$$

Now, the mass of the nitric acid in the tank is given by

$$M_s = \left[\frac{P_1}{gl_c}\right] ft \quad . \tag{3.20}$$

Since SNM is present in the solution at 6 kg-SNM/m^3-solution and the solution density is roughly 1000 kg/m^3 (the density of water) we can say

$$M_s = \alpha M \tag{3.21}$$

where

$\alpha = \frac{1000}{6} = 167$ (kg-solution/kg-SNM), and

M = mass of SNM.

So, substituting into Eq. (3.19) gives

$$\Delta M = \left(\frac{\Delta P_1}{P_1}\right) \alpha M + \left(\frac{\Delta f}{f}\right) M + \left(\frac{\Delta t}{t}\right) M \quad . \tag{3.22}$$

We can see from Eq. (3.22) that SNM mass uncertainties are more sensitive to pressure-reading error than flow rate or time errors, because of the factor, α.

Computing the variance,

$$\boxed{\sigma_{FC}^2 = M^2 \left(\sigma_p^2 + \sigma_f^2 + \sigma_t^2 \right)} \tag{3.23}$$

where

$\sigma_{FC}^2 = E\{\Delta M^2\}$ Fed to the Concentrator

$$\sigma_p^2 = E\left\{\left(\alpha \frac{\Delta P_1}{P_1}\right)^2\right\}$$

$$\sigma_f^2 = E\left\{\left(\frac{\Delta f}{f}\right)^2\right\}$$

$$\sigma_t^2 = E\left\{\left(\frac{\Delta t}{t}\right)^2\right\}$$

Notice that we have lumped the α term into σ_p. We assume that the pressure gauge is accurate enough so that $\sigma_p = 0.1$. We further assume $\sigma_f = 0.1$ and $\sigma_t = 0.01$. Using these values in Eq. (3.23) gives

$$\sigma_{FC} = 5 \text{ kg}\left[(0.1)^2 + (0.1)^2 + (0.01)^2\right]^{1/2}$$

$$\sigma_{FC} = .71 \text{ kg} \tag{3.24}$$

We have completed error analyses for the measurement of (1) SNM mass in the storage tanks and (2) SNM mass fed to the concentrator. We now perform an error analysis on Eq. (3.9), which is the expression for SNM mass removed from the concentrator after a batch run. We consider errors in the two pressure readings, P_1 and P_2. An argument similar to the one presented in Eqs. (3.19) through (3.23) is used, and after some tedious manipulations, the result is

$$\boxed{\sigma_{RC}^2 = M^2 \left(\sigma_{P_1}^2 + \sigma_{P_2}^2 \right)} \tag{3.25}$$

where

σ^2_{RC} = E $\{\Delta M^2\}$ Removed from the Concentrator,

$$\sigma^2_{P_1} = E\left\{(\alpha-\beta)^2\left(\frac{\Delta P_1}{P_1}\right)^2\right\},$$

$$\sigma^2_{P_2} = E\left\{\beta^2\left(\frac{\Delta P_2}{P_2}\right)^2\right\},$$

$\alpha = M_s/M$,

$\beta = M_a/M$,

M_s = mass of solution in the concentrator (kg),

M_a = mass of SNM above the lowest bubbler tube (kg), and

M = mass of SNM in the concentrator (kg).

We assume $\sigma_{P_1} = 0.1$ and $\sigma_{P_2} = 0.1$.

Therefore,

$$\sigma_{RC} = 5 \text{ kg } \left[(0.1)^2 + (0.1)^2\right]^{1/2}$$

$$= 0.71 \text{ kg} \qquad (3.26)$$

Our final measurement is weighing the precipitant cakes. The major source of error here is the lack of knowledge concerning the percentage of water and contaminants in the cakes.

$$\Delta M = - M_{cakes}\Delta b \qquad (3.27)$$

so

$$\boxed{\sigma^2_{WC} = M^2 \sigma^2_b} \qquad (3.28)$$

where

$$\sigma_{WC}^2 = E\{\Delta M^2\} \quad \underline{W}\text{eight of the } \underline{C}\text{akes}$$

$$\sigma_b^2 = E\left\{\left(\frac{M_{cakes}}{M}\,\Delta b\right)^2\right\}$$

We assume $\sigma_b^2 = 0.3$ (i.e., very little is known about the contaminate and water concentration in the cakes).

$$\sigma_{WC} = (5\text{ kg})(0.3)$$
$$= 1.5\text{ kg} \qquad (3.29)$$

Thus concludes our analysis of the four measurement schemes introduced in Section 3.1.4. A summary of our assumed measurement (or guess) uncertainties appears in Table 3.3. We now proceed to characterizing SNM loss detection schemes.

TABLE 3.3. Assumed accuracy of measurements (percentage of full scale).

Measurement	Assumed percentage uncertainty, %	Equivalent SNM mass uncertainty, kg
Tank volume	10	0.5
Solution density	10	0.5
Time	1	0.05
Flow rate	10	0.5
Solution level	10	0.5
Weight of precipitant	30	1.5

Chapter 4

DETECTOR PERFORMANCE AT THE MODEL FACILITY

We wish to evaluate the performance of some simple signal processing techniques for detecting SNM diversion. In Chapter 3, we described an example uranium processing facility and stated the assumptions made concerning plant operation. We now present detector performance evaluation for (1) material balance accounting (MBA), (2) MBA augmented by additional instrumentation on the process units, (3) augmented MBA with multiple, redundant measurements, and (4) diversion detection using a parameterized model of the chemical process.

Detectors are constructed typically of a signal processing algorithm (e.g., averaging) and a decision criteria (e.g., threshold exceeded). (See Fig. 4.1.) The signal processing algorithm is primarily used to obtain or enhance the incoming signal in noise. Once the signals of interest are estimated, a decision function is formed and tested against the decision criteria. MBA is basically a detection technique in which some signal processing could be employed in the form of increasing measurement instrument precision. In MBA the decision functions take different forms (e.g., CUMSUM)[1] and so do the associated decision functions (e.g., V-MASK).[2]

4.1 MATERIAL BALANCE ACCOUNTING

In an MBA scheme for the total facility, the amount of incoming raw material is measured and assayed for uranium content. At the end of processing, the resultant outgoing uranium is weighed, and a check is made to see if the output equals the input.

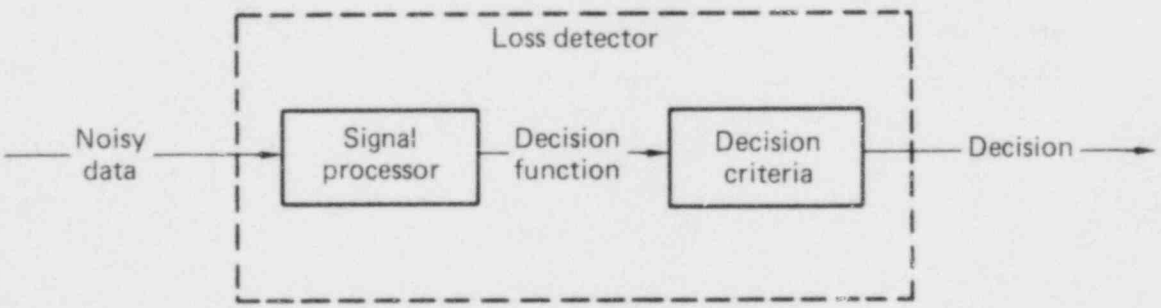

FIG. 4.1. Typical loss detector.

Let us introduce a hypothetical MBA scheme only around the concentrator/precipitator section (Fig. 4.2). The amount of incoming SNM to the concentrator/precipitator section is the amount of SNM in the filled, low-concentration storage tanks. Our uncertainty in the volume of this tank and the density of the solution reflects our uncertainty in the amount of incoming SNM according to Eq. (3.17). Assume that the only measurement of outgoing SNM is the weighing of the wet precipitant cakes. The total error in this accounting is the combination of the input and output measurement errors plus the error associated with natural sources of SNM loss, such as deposit on the inside walls of pipes and tanks.

$$\sigma_{MBA}^2 = \sigma_{ST}^2 + \sigma_{WC}^2 + \sigma_L^2 \tag{4.1}$$

where

σ_{MBA} = MBA loss uncertainty,
σ_{ST} = uncertainty of SNM mass in the storage tanks,
σ_{WC} = uncertainty SNM mass in precipitant cakes, and
σ_L = in-process loss uncertainty (0.2 kg).

Refer to Eqs. (3.17) and (3.28). We are using a tank volume measurement (10 percent error), a solution density measurement (10 percent error), and a weight of precipitant measurement (30 percent error). In addition, all four of the sources of in-process loss listed in Table 3.3 are present in the MBA scheme.

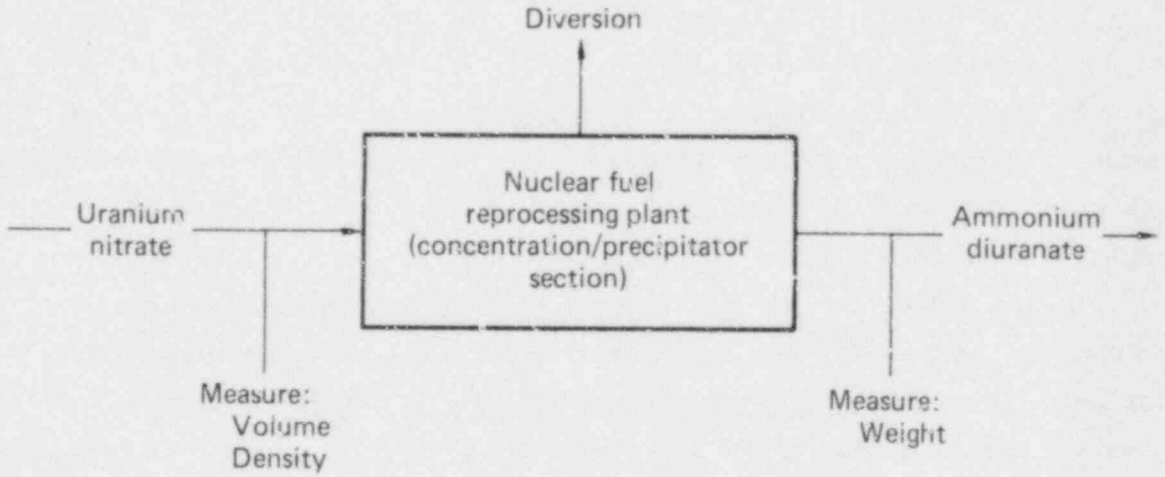

FIG. 4.2. Material balance accounting scheme.

From Eqs. (3.18) and (3.29),

$$\sigma_{MBA} = \left[(0.71)^2 + (1.5)^2 + (0.2)^2\right]^{1/2}$$
$$= 1.67 \text{ kg.} \qquad (4.2)$$

To calculate the probability that the MBA scheme will detect a loss of 1 kg of SNM, we first calculate the signal-to-noise ratio (SNR):

$$SNR = S/\sigma \qquad (4.3)$$

where

$$S = 1 \text{ kg.}$$

Therefore, SNR = 1 kg/1.67 kg = 0.6.

We now refer to the detector performance evaluation curve (Fig. 4.3)* to determine the probability of detection we can expect with a signal-to-noise ratio of 0.6. For the curve shown, we have a fixed probability of false alarm of 0.05. We read that the probability of detection using the MBA scheme is 0.2.

We have concluded our discussion of the MBA loss detection scheme. We now proceed to the signal processing techniques.

4.2 IMPROVED ACCOUNTING USING SIGNAL PROCESSING

We have explained the material balance accounting technique in terms of the concentrator/precipitator section of our model plant. We now introduce three simple signal processing techniques. The first is a multiple-instrument scheme, where process measurements from inside the system are added to the input/output measurements. The second method uses the same instruments as in the multiple-instrument scheme, but it improves the measurement accuracy by calibrating the instruments and taking multiple independent measurements. Calibration reduces the systematic measurement error, the error that is consistent from measurement to measurement. Multiple measurements reduce

---

*This curve is derived mathematically in Appendix A.

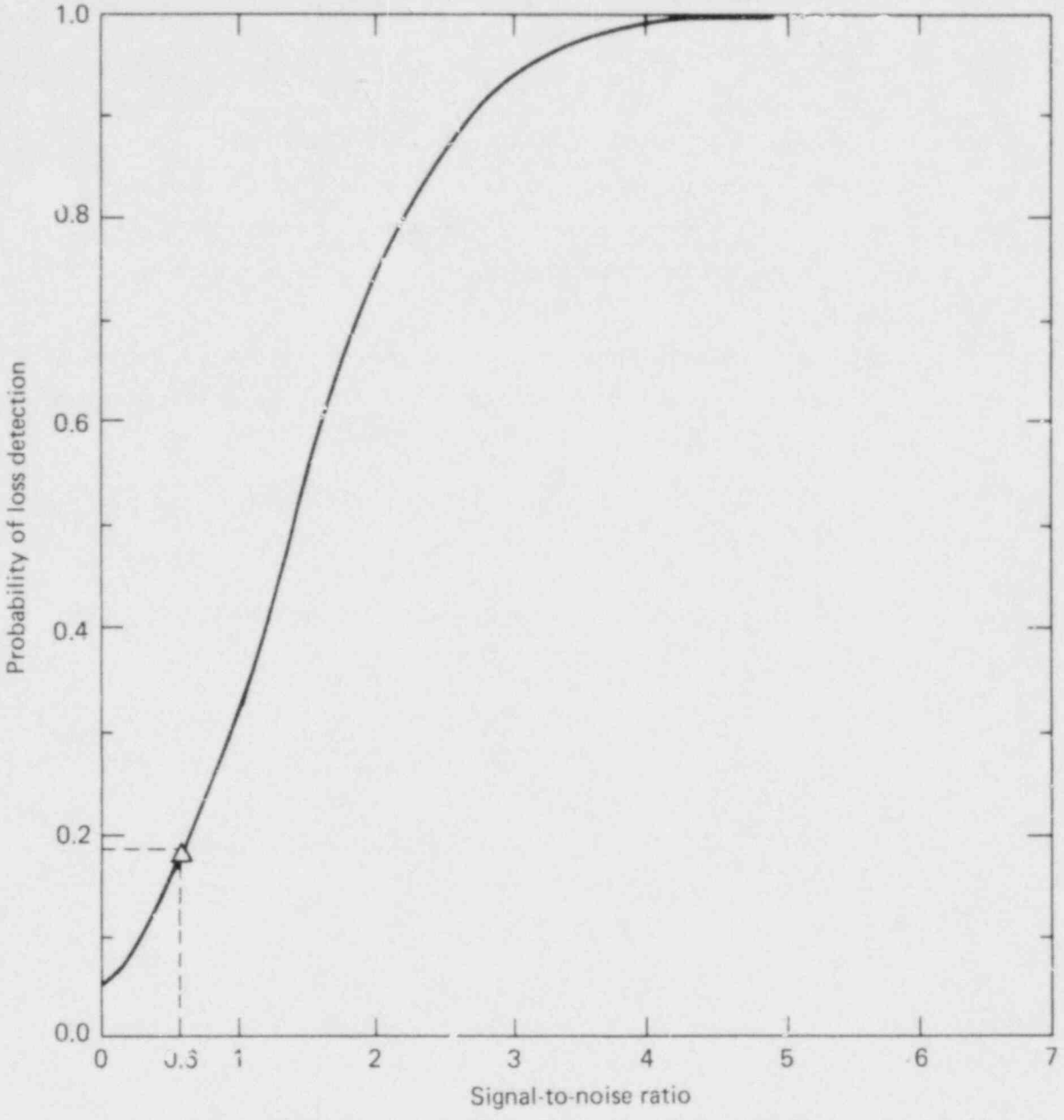

FIG. 4.3. Material balance accounting detector performance (P_F = 0.05).

random measurement error, that error which varies randomly from measurement to measurement. The third scheme is a different approach. We fit measurements of solution density in the concentrator to a linear function of time. The linear function is thus a parameter model of solution concentration.

4.2.1 Multiple Instrument Method

We discuss a signal processing method that utilizes the pressure measurements from the concentrator in addition to the input and output measurements used in MBA. For the sake of discussion, consider a particular scenario: 1 kg of SNM is stolen from the concentrator unit during a batch process (Fig. 4.4).

An estimate of the SNM loss is formed by averaging the measurements of SNM input to the concentrator and subtracting the average of measurements of SNM output from the concentrator:

$$\hat{M}_{LOSS} = \hat{M}_{IN} - \hat{M}_{OUT} \tag{4.4}$$

We apply Eq. (B-14) to form the minimum variance estimates of M_{IN} and M_{OUT}:

$$\hat{M}_{IN} = \left(\frac{M_{ST}}{\sigma^2_{ST}} + \frac{M_{FC}}{\sigma^2_{FC}} \right) \left(\frac{1}{\sigma^2_{ST}} + \frac{1}{\sigma^2_{FC}} \right)^{-1} \tag{4.5}$$

$$\hat{M}_{OUT} = \left(\frac{M_{RC}}{\sigma^2_{RC}} + \frac{M_{WC}}{\sigma^2_{WC}} \right) \left(\frac{1}{\sigma^2_{RC}} + \frac{1}{\sigma^2_{WC}} \right)^{-1} \tag{4.6}$$

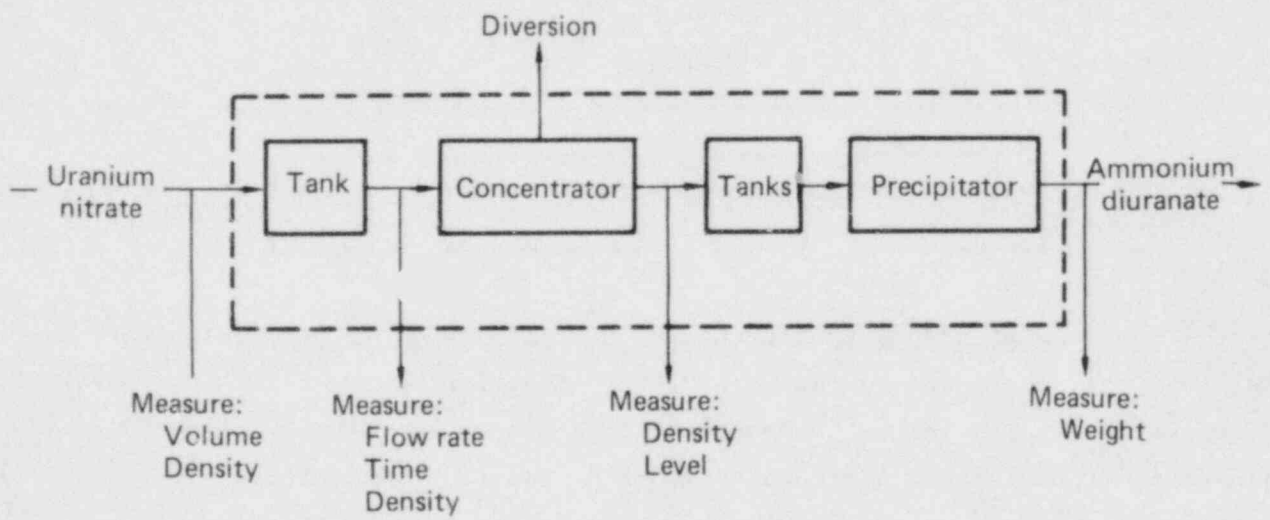

FIG. 4.4. Improved accuracy in material balance accounting.

where

M_{ST} = measured SNM mass in storage tanks,

M_{FC} = measured SNM mass fed to the concentrator,

M_{RC} = measured SNM mass removed from the concentrator, and

M_{WC} = measured SNM mass in the precipitant cakes determined by weighing the cakes.

Using Eq. (B-16), we see that the SNM loss variance is computed by

$$\sigma_{MI}^2 = \left(\frac{1}{\sigma_{ST}^2} + \frac{1}{\sigma_{FC}^2}\right)^{-1} + \left(\frac{1}{\sigma_{RC}^2} + \frac{1}{\sigma_{WC}^2}\right)^{-1} \tag{4.7}$$

where

σ_{MI} = uncertainty in SNM accounting associated with the Multiple Instrument scheme.

Substituting for each σ in Eq. (4.7), using Eqs. (3.18), (3.24), (3.26), and (3.29), results in

$$\sigma_{MI} = 0.79 \text{ kg} \tag{4.8}$$

Figure 4.5 shows that our multiple-instrument method is a modified material balance accounting. Improvement over simple MBA is possible because two separate measurements are taken to estimate SNM entering the concentrator and two measurements to estimate SNM leaving the concentrator.

For a diversion of 1 kg, the signal-to-noise ratio is

$$SNR = \frac{S}{\sigma_{MI}} = (1 \text{ kg})/(0.79 \text{ kg}) = 1.27 \tag{4.9}$$

Figure 4.6 shows where the multiple-instrument scheme lies on the detector evaluation curve. With a SNR of 1.27, the probability of detection is 0.4. In other words, the additional measurements have doubled the detection probability over the simple MBA scheme.

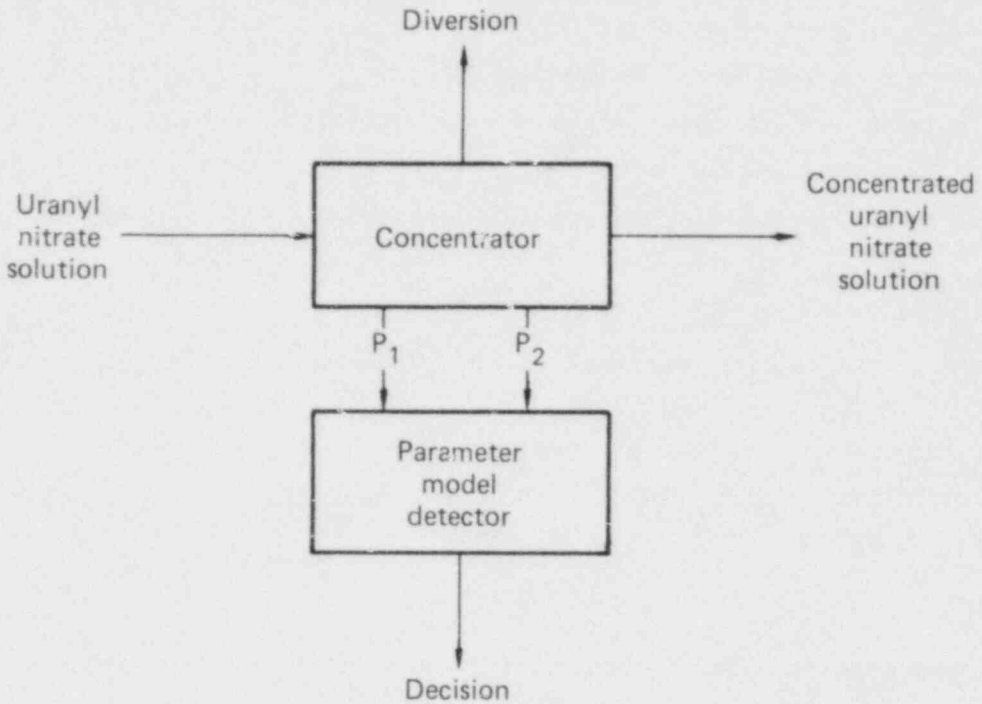

FIG. 4.5. Parameter model diversion detection scheme.

4.2.2 Multiple Measurement Method

We can improve instrument accuracy through redundant measurements. Assume the same scenario and instrument setup as for the multiple-instrument method. We now take many independent readings (say ten) from each instrument and average them. We can expect the signal-to-noise ratio to increase by a factor of 3.162 (the square root of ten) over the multiple-instrument (single measurement) scheme because the noise standard deviation is reduced by this factor when we average the measurements. Thus, the SNR for the multiple measurement scheme is $1.27 \times 3.162 = 4.02$. Note from Fig. 4.6 that the probability of detection has increased from 0.4 to 0.97, a substantial improvement.

4.2.3 Parameter Modeling

A different approach to diversion detection is to model the chemical process as a function of time and, from taking measurements periodically, determine if the data fit the model. A mismatch indicates diversion. Their values can describe a straight line, exponential or other function.

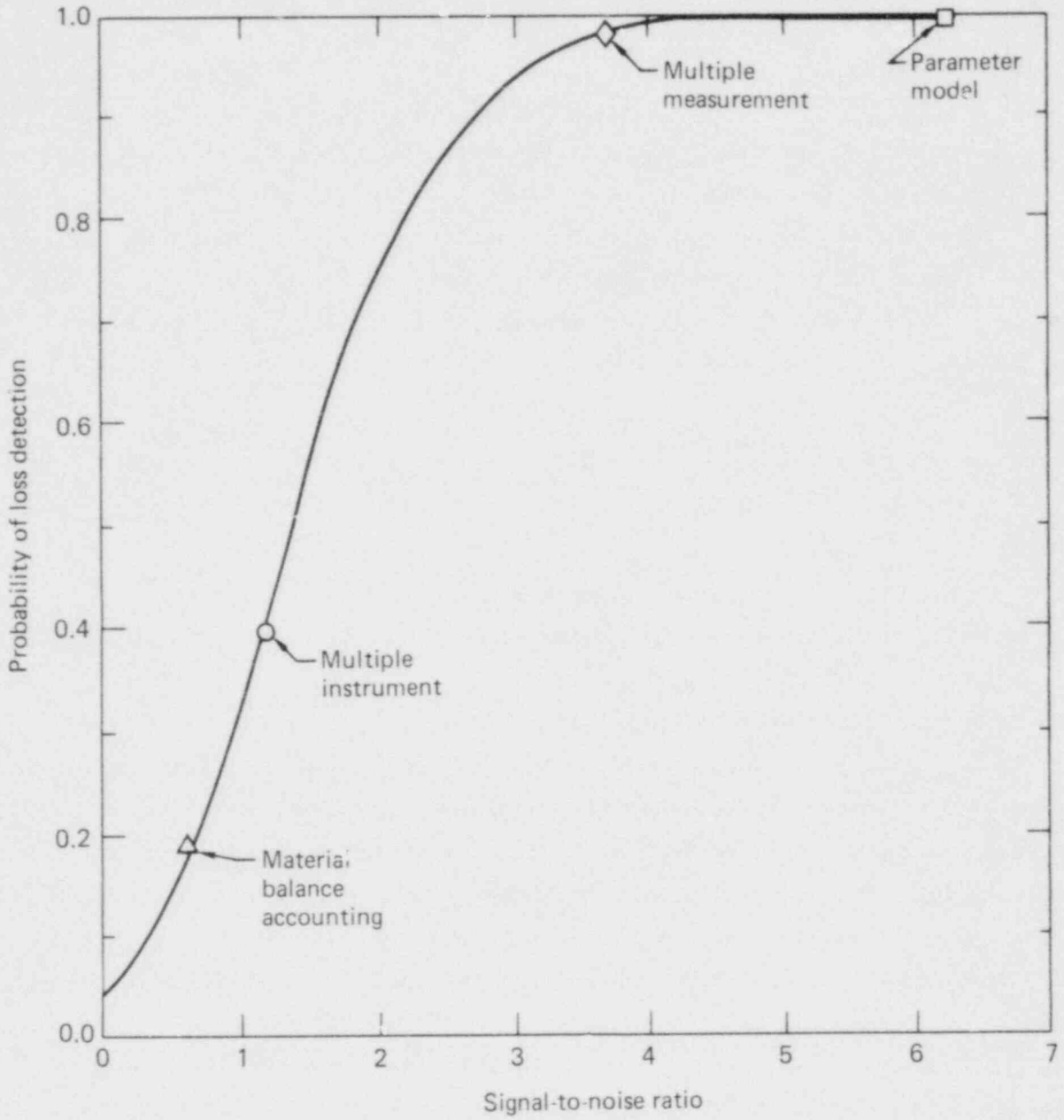

FIG. 4.6. Detector performance evaluation (P_F = 0.05).

For our example, we have chosen to represent the solution density in he concen'rator unit with a li'ear parametric model. The differential pressure gauge provides us with direct measurements of concentration via Eq. (3.10), which is repeated below:

$$c = \frac{P_1}{gl_d} - \sigma_s \tag{4.10}$$

Concentration increases linearly with time during a concentrator run because 6 kg/m^3 solution continues to flow into the concentrator to offset the loss of liquid due to evaporation. Thus, the volume of solution remains constant while SNM continues to pour in at the rate $r = fc_o$ where f is the flow rate (m^3/hr) and c_o is the SNM concentration of the input stream (6 kg SNM/m^3 solution). So we have

$$C(t) = c_o + \left(\frac{rt}{V}\right) \tag{4.11}$$

where

c_o = initial concentration (6 kg SNM/m^3),
r = SNM mass input flow rate (kg/hr),
V = volume of concentrator (m^3), and
t = time since start of batch run.

We use several measurements of concentration [using Eq. (4.10)] during the batch run as data to estimate the parameter, r/V. Let us denote this parameter as $\dot{c}$, the time derivative of the concentration of SNM in the concentrator. In our model plant, to increase concentration from 6 kg/m^3 to 100 kg/m^3 during a 7-hour batch run, the nominal value of $\dot{c}$ is about 13.5 kg/m^3 hr. If $\dot{c}$ deviates from the nominal value, then diversion can be presumed.

The estimator for $\dot{c}$ is called a straight-line-fit algorithm. Smith [3] provides an excellent derivation of the straight-line-fit algorithm. We present here the resulting variance in the estimate of $\dot{c}$:

$$\sigma^2 = \left(\frac{12}{nT^2}\right)\sigma_c^2 \tag{4.12}$$

where

σ^2 = variance of the r/V parameter estimate,
σ_c^2 = variance in the periodic measurements of solution concentration,
T = total batch run time (7 hr), and
n = number of periodic measurements of concentration during the batch run.

Let us assume that we are measuring solution density in the concentrator using an improved accuracy scheme. That is, we have calibrated the pressure meter and we take multiple independent readings to reduce random error. Ten independent readings at one point in time will reduce the solution density error variance by a factor of ten, so we have

$$\sigma_d^2 = (0.5 \text{ kg})^2/10 \tag{4.13}$$

The 0.5 kg SNM mass uncertainty is due to the inaccuracy of ascertaining solution density with a single pressure reading (Table 3.3). We perform this improved-accuracy measurement once every half-hour during the 7-hour batch process, for a total of n = 15 measurements. Therefore, the variance in the estimate of the density rate, $\dot{c}$, is

$$\sigma^2 = \frac{12}{(15)(7 \text{ hr})^2} (0.5 \text{ kg})^2/10$$

or

$$\sigma = 0.02 \text{ kg/hr} \tag{4.14}$$

The signal, S, is the diversion of 1 kg of SNM over a period of 7 hours:

$$S = 1 \text{ kg}/7 \text{ hr} = 0.14 \text{ kg/hr} \tag{4.15}$$

Thus the signal-to-noise ratio is

$$SNR = S/\sigma = 7.0 \tag{4.16}$$

The straight-line-fit algorithm offers a signal-to-noise ratio of 7.0 for a 1-kg diversion. From the graph in Fig. 4.6, we can see that the probability of detection is very close to 1.

Chapter 5

SUMMARY

Using the concentrator/precipitator section of a model scrap uranium processing plant as an example, we have characterized four SNM diversion detection schemes. Each subsequent detector scheme described in this report offers a succeedingly greater signal-to-noise ratio and thus a better probability of detection. Table 5.1 summarizes these results. The maximum time to detection corresponds to the batch processing time of 8 hours.

A large increase in detection probability occurs when the multiple measurements scheme is used. The parameter model and the dynamic models (in future work) will almost certainly detect a diversion of 1 kg of SNM.

TABLE 5.1. Detector performance.[a,b]

Scheme	Signal-to-noise ratio	Probability of loss detection
MBA	0.6	0.2
Multi-Instrument	1.27	0.4
Multi-Measurement	4.0	0.97
Parameter Model	7.0	0.99

[a] Diversion is 1 kg from a 5-kg batch process.

[b] P_F = Probability of false alarm = 0.05.

T_D = Time to detection = 8 hours (batch process time).

Chapter 6

FUTURE WORK

The logical extension to this report is the investigation of some on-line process monitors that utilize dynamic models for each of the chemical units. These on-line detectors will utilize a signal processing algorithm (e.g., Kalman filter) to process the incoming measurements. The chemical processes, themselves, will be modeled by multistate differential equations.

As was mentioned earlier, on-line detection offers the distinct advantage of providing a timely detection of diversion. It can provide estimates of chemical process parameters that are not or cannot be measured directly and this can lead to a quick localization of the loss. We also expect the on-line monitors to be sensitive to a wide range of adversary actions that otherwise might have gone undetected in MBA schemes.

Additional contents of a future report will be a cost-benefit tradeoff analysis. Simple signal processing may offer a great increase in benefits at a low cost; however, the increase in benefits of more complex schemes will need to be carefully weighted against cost factors.

GLOSSARY

Probability Density is a function of a continuous random variable, X. The random variable may assume a value between x and x + Δx with probability $P_x(x)\ \Delta x$ (Δx is assumed to be very small). $P_X(x)$ is called the Probability Density Function (PDF) for the random variable (RV), X.

Gaussian is the characteristic probability density function of most types of random noise. The value of the noise may vary over a wide range. The probability density over that range is a "bell" or "normal" curve:

$$P_x(x) = \frac{1}{\sqrt{2\pi}\sigma_x} \exp \left\{ -\frac{1}{2} (x - m_x)^2 \Big/ \sigma_x^2 \right\}$$

Mean is the average value (also called expected value) for a random variable. Mathematically,

$$m_x = E\{x\} = \int_{-\infty}^{\infty} x\, P_X(x)\, dx$$

Variance is the average squared deviation from the mean of random variable:

$$\sigma_x^2 = E\{(x - m_x)^2\} = \int_{-\infty}^{\infty} (x - m_x)^2\, P_x(x)\, dx$$

The variance can be considered the "spread" of possible values for X or the "width" of the probability density function.

Standard deviation is the square root of the variance. It is also called uncertainty.

REFERENCES

1. John L. Jaech, Statistical Methods in Nuclear Material Control, U.S. Atomic Energy Commission, 1973.
2. M. A. Wincek, K. B. Stewart, and G. F. Piepel, Statistical Methods for Evaluating Sequential Material Balance Data, Battelle Pacific Northwest Laboratory, PNL-29_0, 1979.
3. J. M. Smith, Analysis of Inertial Navigation Systems, Rockwell International, X79-60/201, 1979, pp. VIII-2-11.

RHM/cs

Appendix A

DETECTION THEORY OVERVIEW

Detection is the process of deciding between two (or more) alternatives using whatever information is available. In the specific application to nuclear safeguards, the alternatives, hereafter called hypotheses, are (1) the situation is normal, the nuclear material is accounted for; and (2) the situation is abnormal, some material has been lost.

In this appendix, we discuss the binary hypothesis (two alternative) detector, define some terms, and introduce detector performance measures. We then describe the signal processing role in detection schemes. With this background, we derive an evaluation curve to explain how detector performance is related to the quality of the signal processing.

We assume that a set of measurements, $\underline{z}$, is available and we wish to decide between two hypotheses:

$$H_o: \quad \underline{z} = \underline{v}$$
$$H_1: \quad \underline{z} = \underline{h}x + \underline{v} \qquad \text{(A-1)}$$

$\underline{z}$ is the n-vector of measurements (i.e., a set of n separate measurements), $\underline{v}$ is an n-vector of measurement errors (random noise), x is a scalar quantity (for our example, x represents the amount of lost SNM in a diversion scenario), and $\underline{h}$ is an n-vector linearly relating the signal, x, to the set of measurements, $\underline{z}$.

Let us define a few terms associated with detectors. Probability of detection (P_D) is the probability that the detector will choose H_1 when H_1 is, in fact, correct. Probability of false alarm (P_F) is the probability that the detector will choose H_1 incorrectly; i.e., when H_o is the true case.

We have n measurements. The set of all possible measurements will therefore span an n-dimensional space. The n-space is divided into two regions: R_o, associated with hypothesis zero, and R_1, associated with hypothesis one (Fig. A-1). The detector's task is to determine which region $\underline{z}$ lies in.

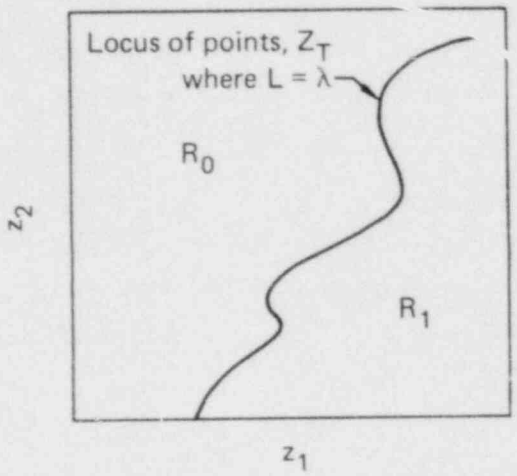

FIG. A-1. Decision regions.

To design the detector, we specify the regions that satisfy the following condition: the probability of detection is maximized while the probability of false alarm is constrained to some chosen, low, value.

The detection and false alarm probabilities are

$$P_D = \int_{R_1} p(\underline{z} \mid H_1) d\underline{z} \tag{A-2}$$

$$P_F = \int_{R_1} p(\underline{z} \mid H_o) d\underline{z} \tag{A-3}$$

where $p(\underline{z}|H_1)$ is the joint probability density function PDF) of the measurement vector, $\underline{z}$, in the case where H_1 is true, and $p(\underline{z}|H_o)$ is the PDF for $\underline{z}$ when H_o is true. The integrals represent multidimensional integration over region R_1. We choose the region, R_1, which maximizes P_D, while keeping $P_F \leq \gamma$, where γ is some (chosen) constant. The solution to this design problem* is to choose a border between the two regions, R_o and R_1, such that the likelihood ratio is a constant:

$$L = \frac{p\ (z_T|H_1)}{p\ (\underline{z}_T|H_o)} = \lambda \tag{A-4}$$

$\underline{z}_T$ represents the locus of points defining the border between R_o and R_1. λ is a factor dependent on γ, which is the upper limit on the False Alarm

*Andrew P. Sage and James L. Melsa, Estimation Theory With Applications to Communications and Control (McGraw Hill Book Company, Inc., New York), 1971.

probability. We must adjust λ until $P_F = \gamma$. (Note that we have had to hit the bound of our constraint, $P_F \leq \gamma$, in order to maximize P_D. The reason for this is that Eqs. (A-2) and (A-3) are integrations over the same region, and both probabilities increase monotonically with the size of that integration region).

We mentioned that the detector must determine which region $\underline{z}$ lies in. The detector performs a likelihood ratio test. In region R_1, the likelihood ratio is always greater than λ; in region R_2, the ratio is always less than λ:

$$L = \frac{p\ (\underline{z}|H_1)}{p\ (\underline{z}|H_o)} \quad \begin{cases} > \lambda : \underline{z} \in R_1, \text{ choose } H_1 \\ < \lambda : \underline{z} \in R_o, \text{ choose } H_o \end{cases}$$

For example, consider the special case where the PDFs are Gaussian:

$$p\ (\underline{z}|H_o) = \frac{1}{(2\pi)^{n/2} \mid R \mid^{1/2}} \exp\ \left\{-1/2\ \underline{z}^T\ R^{-1}\ \underline{z}\right\} \tag{A-5}$$

$$p\ (\underline{z}|H_1) = \frac{1}{(2\pi)^{n/2} \mid R \mid^{1/2}} \exp\ \left\{-1/2\ (\underline{z} - \underline{h}x)^T\ R^{-1}\ (\underline{z} - \underline{h}x)\right\} \tag{A-6}$$

where

$$R = E\left\{\underline{v}\ \underline{v}^T\right\}$$

The likelihood ratio is

$$L = \frac{\exp\ \left\{-1/2\ \left(\underline{z}_T - \underline{h}x\right)^T\ R^{-1}\ \left(\underline{z}_T - \underline{h}x\right)\right\}}{\exp\ \left\{-1/2\ \underline{z}_T R^{-1} \underline{z}_T\right\}}$$

$$= \exp\ \left\{-1/2\ \left[-\underline{z}_T^T R^{-1} \underline{h}x - x\underline{h}^T\ R^{-1}\ \underline{z}_T + x\underline{h}^T R^{-1}\ \underline{h}\ x\right]\right\}$$

$$= \exp\ \left\{x\ (\underline{h}^T\ R^{-1}\ \underline{h})\left[\left(\underline{h}^T\ R^{-1}\ \underline{h}\right)^{-1} \underline{h}^T R^{-1}\ \underline{z}_T - 1/2\ x\right]\right\} \tag{A-7}$$

Constraining L to be constant on the border between R_o and R_1 constrains the term in brackets in Eq. (A-7) to be constant, so, by this requirement, $\underline{z}_T$ describes a "hyperplane" in $\underline{z}$ space:

$$(\underline{h}^T R^{-1} \underline{h})^{-1} h^T R^{-1} \underline{z}_T - 1/2\ x = C \qquad \text{(A-8)}$$

where C is the constant

$$C = \ln(\lambda) - x^{-1} (\underline{h}^T R^{-1} \underline{h})^{-1}$$

If $\underline{z}$ lies to one side of the hyperplane defined by Eq. (A-8) (in the region containing $\underline{z} = 0$) the detector chooses H_o. On the other side of the hyperplane, the detector chooses H_1.

Now let us discuss the application of signal processing to a detection scheme. By signal processing we imply that the set of measurements, $\underline{z}$, will be "processed" to form another number, say $\hat{x}(\underline{z})$, which alone is sufficient for deciding the region in which $\underline{z}$ lies.

Let us define $\hat{x}$ so that the hypothesis test is

$$\begin{aligned} H_o &: \hat{x}(\underline{z}) = \tilde{x} \\ H_1 &: \hat{x}(\underline{z}) = x + \tilde{x} \end{aligned} \qquad \text{(A-9)}$$

where x is the true amount of SNM stolen and $\tilde{x}$ is a random error.

To show that this hypothesis test is identical to the previous hypothesis test, Eq. (A-1), we must show that the associated likelihood ratios are identical for any given set of measurements, $\underline{z}$.

We choose $\hat{x}(k)$ to be the minimum variance estimate (Appendix B) of x, given the measurements, $\underline{z}$:

$$\hat{x}(z) = (\underline{h}^T R^{-1} \underline{h})^{-1} h^T R^{-1} \underline{z} \qquad \text{(A-10)}$$

We now assume the special case, once again, where $\underline{z}$ has a Gaussian PDF under either hypothesis. $\hat{x}(z)$ in (A-10) can be shown to also have a Gaussian PDF.** Therefore, $\tilde{x}$ (defined to be $\hat{x}$ under H_o, and $\hat{x}$-x under H_1) has a Gaussian PDF. In Appendix B, we show that $\tilde{x}$ has the variance

$$E\{\tilde{x}^2\} \triangleq \sigma_x^2 = (\underline{h}^T R^{-1} \underline{h})^{-1} \qquad \text{(A-11)}$$

**Athanasios Papoulis, Probability, Random Variables, and Stochastic Processes (McGraw-Hill Book Company, Inc., New York), 1965.

Now we form the likelihood ratio

$$L = \frac{p\ (\hat{x}\ (\underline{z}) \mid H_1)}{p\ (\hat{x}\ (\underline{z}) \mid H_o)}$$

$$= \frac{\exp\ \{-1/2\ (\hat{x} - x)^2/\sigma_x^2\}}{\exp\ \{-1/2\ \hat{x}^2/\sigma_x^2\}}$$

$$L = \exp\ \{x\ \sigma_x^{-2}\ (\hat{x} - 1/2\ x)\} \qquad \text{(A-12)}$$

Equation (A-12) is identical to (A-7) when we make the substitutions of (A-10) and (A-11), therefore, the hypothesis test is the same using either the full set of measurements, $\underline{z}$, or the sufficient statistic, $\hat{x}$.

What we have shown is that we can break up the detection process into two steps: first, the signal processing where $\hat{x}(\underline{z})$ is computed, then the hypothesis test on $\hat{x}$. The advantage is that now, after signal processing, the likelihood ratio is simpler to compute (for a given amount of stolen material, x) because the PDFs are functions of a single variable, $\hat{x}$, instead of n variables, $\underline{z}$ (Fig. A-2). Also, we find it much easier to compute P_D and P_F. Before, they were multidimensional integrations (A-2) and (A-3), now they are single integrals:

$$P_D = \int_{x_T}^{\infty} p\ (\hat{x} \mid H_1)\ d\ \hat{x} \qquad \text{(A-13)}$$

$$P_F = \int_{x_T}^{\infty} p\ (\hat{x} \mid H_o)\ d\ \hat{x} \qquad \text{(A-14)}$$

where x_T is chosen such that $P_F = \gamma$ (x_T is called the detection threshold).

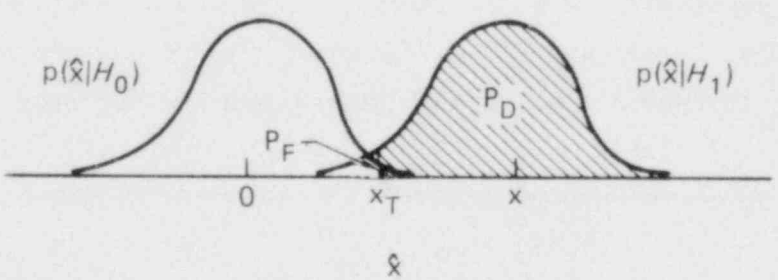

FIG. A-2. Probability density functions for x.

We also find that the hypothesis test is greatly simplified. Instead of using the likelihood ratio test, we can simply decide if $\hat{x}$ is greater or less than x_T, the detection threshold:

if $\hat{x} > x_T$ choose H_1
if $\hat{x} < x_T$ choose H_o

Let us now characterize the detection scheme we have designed. The probability of detection is commonly used as one measure of performance for detector schemes. Consider the equation for P_D (A-13) in the Gaussian case:

$$P_D = \int_{x_T}^{\infty} \frac{1}{\sqrt{2\pi}\,\sigma_x} \exp\left\{-1/2\ (\hat{x} - x)^2/\sigma_x^2\right\} d\,\hat{x}$$

We introduce a change of variables:

$$\alpha = (\hat{x} - x)/\sigma_x$$

We now have

$$P_D = \int_{(x_T - x)/\sigma_x}^{\infty} \frac{1}{\sqrt{2\pi}} \exp\left\{-1/2\ \alpha^2\right\} d\alpha$$

$$P_D = 0.5 + \text{erf}\left[(x - x_T)/\sigma_x\right] \qquad \text{(A-15)}$$

where erf or error function is defined as[2]

$$\text{erf}\ (y) \triangleq \int_o^y \frac{1}{\sqrt{2\pi}} \exp\left\{-1/2\ \alpha^2\right\} d\alpha. \qquad \text{(A-16)}$$

Note that the probability of detection depends upon x_T, the chosen threshold, and x, the amount of material stolen in a diversion scenario.

Another measure of detector performance is the false alarm probability, P_F. Using Eq. (A-14) with a Gaussian PDF,

$$P_F = \int_{x_T}^{\infty} \frac{1}{\sqrt{2\pi}\sigma} \exp\left\{-1/2\ \hat{x}^2/\sigma_x^2\right\}\ d\hat{x}. \qquad \text{(A-17)}$$

Once again we introduce a change of variables:

$$\beta = \hat{x}/\sigma_x$$

so that

$$P_F = \int_{x_T/\sigma_x}^{\infty} \frac{1}{\sqrt{2\pi}} \exp\left\{-\ 1/2\ \beta^2\right\}\ d\beta. \qquad \text{(A-18)}$$

Using the above definition of error function, we have

$$P_F = 0.5 + \text{erf}\ (-\ x_T/\sigma_x). \qquad \text{(A-19)}$$

Note that probability of false alarm also depends upon the chosen threshold, x_T. By comparing Eq. (A-19) with Eq. (A-15), we can conclude that the probability of false alarm is equal to the probability of "detecting" a loss of zero material. This is to be expected because, when $x = 0$, the PDFs for hypothesis one and hypothesis zero coincide. For the purposes of this report, we are not concerned with the case where x (an amount of stolen material) is less than zero.

For our example, we chose a detection threshold, x_T, such that $P_F = 0.05$. In this case,

$$x_T = 1.6\ \sigma_x. \qquad \text{(A-20)}$$

Substituting Eq. (A-20) into Eq. (A-15),

$$P_D = 0.5 + \text{erf}\ \left[x/\sigma_x - 1.6\right] \qquad \text{(A-21)}$$

The function in Eq. (A-21) is plotted in Fig. A-3. We call the factor, x/σ_x, the signal-to-noise ratio (SNR). Note that the "noise," σ_x, is the

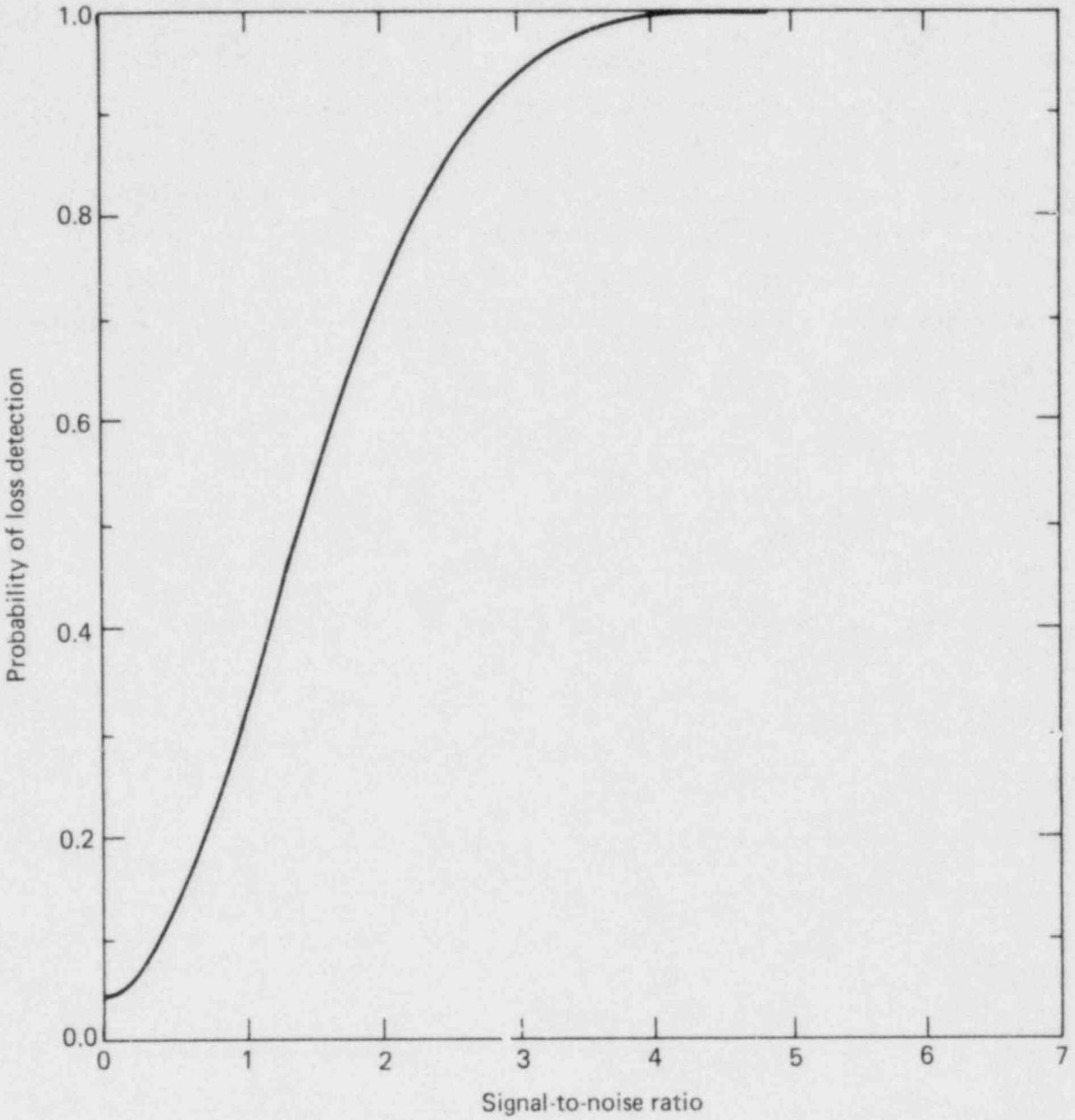

FIG. A-3. Probability of loss detection versus signal-to-noise ratio (P_F = 0.05).

Standard deviation of the error in estimating the "signal," x. In other words, the noise, and thereby the detector performance, in terms of P_D, is directly dependent on the quality of the signal processing algorithm. The plot in Fig. A-3 can be considered a detector performance evaluation curve. The better detectors have a higher probability of detection; therefore, their signal processing schemes must have an inherently higher signal-to-noise ratio. SNR is a key factor in designing a signal processing/detection system.

Appendix B

CALCULATION OF A MINIMUM VARIANCE ESTIMATE

When many measurements of various degrees of accuracy are available for estimating a single parameter, the minimum variance technique provides the "best" solution. The "best" solution is the estimate, which, on the average, has the least-squared deviation from the true parameter's value. The problem is to minimize:

$$J = E\left\{(x - \hat{x})^2\right\} \tag{B-1}$$

where x is the parameter

$\hat{x}$ is the estimate.

Each measurement of the parameter is corrupted by some additive error:

$$z_i = x + \varepsilon_i \tag{B-2}$$

($i = 1,\ldots, n$; n equals the total number of measurements).

The errors are Gaussian random variables:

$$E\left[\varepsilon_i\right] = 0$$
$$E\left[\varepsilon_i^2\right] = \sigma_i^2 \tag{B-3}$$

In vector notation, Eq. (B-2) can be written as

$$\underline{z} = H\,x + \underline{\varepsilon} \tag{B-4}$$

where

$$\underline{z} = \begin{bmatrix} z_1 \\ \vdots \\ z_n \end{bmatrix}, \quad H = \begin{bmatrix} 1 \\ \vdots \\ 1 \end{bmatrix}, \quad \underline{\varepsilon} = \begin{bmatrix} \varepsilon_1 \\ \vdots \\ \varepsilon_n \end{bmatrix}$$

The most convenient form for an estimate of x is some linear combination of the measurements:

$$\hat{x} = \sum_{i=1}^{n} k_i z_i = K\underline{z} \tag{B-5}$$

where $K = \left[k_1, \ldots k_n \right]$ and a constraint on the estimate is that it be unbiased, i.e.,

$$E\ (\hat{x} - x) = 0$$

or

$$E(\hat{x}) = x. \tag{B-6}$$

where $E(\cdot)$ denotes statistical expected value.

$$E(K\underline{z}) = x$$

$$E(KHx + K\underline{\epsilon}) = x$$

$$KHx = x$$

which implies

$$KH = I \tag{B-7}$$

To reflect the above constraint in the minimization of Eq. (B-1), we will use the Lagrange multiplier technique:

$$J = E\left\{(x - \hat{x})^2\right\} + \lambda(I - KH). \tag{B-8}$$

J is to be minimized with respect to a choice of K and λ, so

$$\frac{\partial J}{\partial \lambda} = 0$$

and

$$\frac{\partial J}{\partial K} = 0 \tag{B-9}$$

are required

$$J = E\left\{(x - K\underline{z})^2\right\} + \lambda(I - KH)$$

$$= E\left\{(x - KHx - K\underline{\epsilon})^2\right\} + \lambda(I - KH)$$

$$J = x^2 - 2KHx^2 + KHH^TK^Tx^2 + KRK^T + \lambda(I - KH) \tag{B-10a}$$

where $R = E\,\underline{\epsilon}\,\underline{\epsilon}^T$ (B-10b)

$$= \begin{bmatrix} \sigma_1^2 & & \\ & \ddots & \\ & & \sigma_n^2 \end{bmatrix}$$

Now

$$\frac{\partial J}{\partial \lambda} = I - KH = 0 \tag{B-11a}$$

and

$$\frac{\partial J}{\partial K} = -2Hx^2 + 2HH^TK^Tx^2 + 2RK^T - \lambda H = 0 \tag{B-11b}$$

Solving Eq. (B-11b) for K (and using the fact that KH = 1),

$$K = \frac{1}{2}\lambda H^T R^{-1} \tag{B-12}$$

To determine λ, we substitute Eq. (B-12) into Eq. (B-11a):

$$I = \frac{1}{2}\lambda H^T R^{-1} H = 0$$

$$\frac{1}{2}\lambda = (H^T R^{-1} H)^{-1}$$

So Eq. (B-12) becomes

$$K = (H^T R^{-1} H)^{-1} H^T R^{-1} \tag{B-13}$$

Substitute for H and R^{-1} in Eq. (B-13) using Eqs. (B-4) and (B-10b):

$$\hat{x} = K\underline{z} = \left([1 \ldots 1] \begin{bmatrix} \sigma_1^{-2} & & \\ & \ddots & \\ & & \sigma_n^{-2} \end{bmatrix} \begin{bmatrix} 1 \\ \vdots \\ 1 \end{bmatrix} \right)^{-1} [1 \ldots 1] \begin{bmatrix} \sigma_1^{-2} & & \\ & \ddots & \\ & & \sigma_1^{-2} \end{bmatrix} \begin{bmatrix} z_1 \\ \vdots \\ z_n \end{bmatrix}$$

$$\boxed{\hat{x} = \frac{\sum_{i=1}^{n} z_i / \sigma_i^2}{\sum_{i=1}^{n} 1 / \sigma_i^2}} \tag{B-14}$$

Equation (B-14) shows that in order to estimate x, the measurements, z_i, must be inverse-weighted by their respective accuracies, σ_1^2, and added together. The result is then normalized by the sum of the weights.

The accuracy of the estimate is usually of interest, so we shall compute

$$\sigma_e^2 = E\left\{ [\hat{x} - E(\hat{x})]^2 \right\}$$

or

$$\sigma_e^2 = E(\hat{x}^2) - [E(\hat{x})]^2$$

$$= E\left\{ (KHx - K\underline{\epsilon})^2 \right\} - x^2$$

since KH = I

$$\sigma_e^2 = E\left\{ (x - K\underline{\epsilon})^2 \right\} - x^2$$

$$\sigma_e^2 = KRK^T$$

where $R = E[\underline{\epsilon}\ \underline{\epsilon}^T]$.

Substituting Eq. (B-13) into the above gives

$$\sigma_e^2 = \left(H^T R^{-1} H\right)^{-1} H^T R^{-1} R R^{-1} H \left(H^T R^{-1} H\right)^{-1}$$

$$= \left(H^T R^{-1} H^{-1}\right) \quad . \tag{B-15}$$

Substituting for H and R gives

$$\boxed{\sigma_e^2 = \frac{1}{\sum_{i=1}^{n} 1/\sigma_i^2}} \tag{B-16}$$

As an example of how the minimum variance estimate is related to the common notion of averaging, consider the case when all the measurement accuracies are the same:

$$\sigma_i = \sigma \qquad i = 1,\ldots,n$$

Equation (B-14) becomes

$$x = \frac{\sum_{i=1}^{n} z_i/\sigma^2}{\sum_{i=1}^{n} 1/\sigma^2} = \frac{\frac{1}{\sigma^2} \sum_{i=1}^{n} z_i}{\frac{n}{\sigma^2}} = \frac{1}{n} \sum_{i=1}^{n} z_i \quad ,$$

which is the common "average."

Equation (B-16), for the variance, becomes

$$\sigma_e^2 = \frac{1}{\sum_{i=1}^{n} 1/\sigma^2} = \frac{1}{n/\sigma^2} = \frac{\sigma^2}{n}$$

which is also well known as the fact that variance decreases proportional to n, the number of measurements taken.

Appendix C

LINEARIZATION TECHNIQUE FOR ERROR ANALYSIS

Many quantities of interest in a system may be a function of several uncertain parameters, x_i:

$$y: = f(x_1, x_2, \ldots, x_n) \triangleq f(\underline{x})$$

The uncertainty in y due to uncertainty in $\underline{x}$ would most easily be computed if f were a linear function of $\underline{x}$; however, there are many important applications for error analysis where f is highly nonlinear. In these cases, f can be approximated as a linear function in a small region about a nominal point, $\underline{x}_0$.

Assuming f(x) is well-behaved in the vicinity of $\underline{x}_0$, f can be expanded in a Taylor series:

$$\begin{aligned} y_0 + \Delta y &= f(\underline{x}_0 + \Delta\underline{x}) \\ &= f(\underline{x}_0) + \sum_{\alpha=1}^{n} \frac{\partial f}{\partial x_\alpha} \Delta x_\alpha \\ &+ \frac{1}{2} \sum_{\alpha=1}^{n} \sum_{\beta=1}^{n} \frac{\partial^2 f}{\partial x_\alpha \partial x_\beta} \Delta x_\alpha \Delta x_\beta \\ &+ \frac{1}{3!} \sum_{\alpha=1}^{n} \sum_{\beta=1}^{n} \sum_{\gamma=1}^{n} \frac{\partial^3 f}{\partial x_\alpha \partial x_\beta \partial x_\gamma} \Delta x_\alpha \Delta x_\beta \Delta x_\gamma \\ &+ \ldots \end{aligned} \tag{C-1}$$

Equation (C-1) can be made linear in $\Delta\underline{x} = (\Delta x_\alpha, \alpha=1,\ldots,n)$ if it is assumed Δx_α is small enough that terms on the order of $\Delta x_\alpha \Delta x_\beta$ are insignificant. Then,

$$y_0 + \Delta y \cong f(x_0) + \sum_{\alpha=1}^{n} \frac{\partial f}{\partial x_\alpha} \Delta x_\alpha$$

and since $y_0 = f(x_0)$:

$$\boxed{\Delta y \cong \sum_{\alpha=1}^{n} \frac{\partial f}{\partial x_\alpha} \Delta x_\alpha} \qquad \text{(C-2)}$$

Example

$$y = ap^{-1} \ln p$$

$$\Delta y = \frac{\partial y}{\partial \alpha} \Delta a + \frac{\partial y}{\partial_p} \Delta p$$

$$= (p_0^{-1} \ln p_0) \Delta a$$

$$+ (-a_0 p_0^{-2} \ln p_o + a_o p_0^{-2}) \Delta p$$

NRC FORM 335 (7 77)

U.S. NUCLEAR REGULATORY COMMISSION

BIBLIOGRAPHIC DATA SHEET

1. REPORT NUMBER (Assigned by DDC)
NUREG/CR-1785
UCRL-53012

4. TITLE AND SUBTITLE (Add Volume No., if appropriate)
Performance Evaluation of Loss Detection Schemes for Uranium Recovery Plants

2. (Leave blank)

3. RECIPIENT'S ACCESSION NO.

7. AUTHOR(S)
Don T. Gavel

5. DATE REPORT COMPLETED
MONTH: November YEAR: 1980

9. PERFORMING ORGANIZATION NAME AND MAILING ADDRESS (Include Zip Code)
Lawrence Livermore National Laboratory
NSS Safeguards Program: L-97
P.O. Box 808
Livermore, CA 94550

DATE REPORT ISSUED
MONTH: November YEAR: 1981

6. (Leave blank)

8. (Leave blank)

12. SPONSORING ORGANIZATION NAME AND MAILING ADDRESS (Include Zip Code)
Office of Nuclear Regulatory Research
U.S. Nuclear Regulatory Commission
Washington, DC 20555

10. PROJECT/TASK/WORK UNIT NO.

11. CONTRACT NO.
FIN A0115

13. TYPE OF REPORT
Interim Technical Report

PERIOD COVERED (Inclusive dates)

15. SUPPLEMENTARY NOTES

14. (Leave blank)

16. ABSTRACT (200 words or less)

This report presents four loss detection schemes for special nuclear material (SMN) accounting at a typical uranium recovery facility. A detector is defined and loss detector performance evaluation criteria are discussed. The loss detection schemes are evaluated for a hypothetical SNM loss scenario. The schemes presented are (1) material balance accounting (MBA), where single measurements are made of incoming and outgoing SNM; (2) MBA, augmented by additional measurements (i.e., multiple instruments) made on chemical processes within the plant; (3) augmented MBA, with the measurement instruments improved by multiple independent reading; and (4) a detector based on a parameterized model of the chemical process. The results of our analysis show that better process models and improved accuracy measurements can greatly enhance the performance of an SNM diversion detector. Detector performance was evaluated for an 8 hour batch processing time.

17. KEY WORDS AND DOCUMENT ANALYSIS

17a. DESCRIPTORS

Loss detection
SNM Special nuclear material
MBA Accounting
diversion

17b. IDENTIFIERS/OPEN-ENDED TERMS

18. AVAILABILITY STATEMENT
Unlimited

19. SECURITY CLASS (This report)
Unclassified

21. NO. OF PAGES

20. SECURITY CLASS (This page)
Unclassified

22. PRICE
$

NUREG/CR-1785

PERFORMANCE EVALUATION OF LOSS DETECTION SCHEMES FOR URANIUM RECOVERY PLANTS

NOVEMBER 1981